

SEPARATION OF THE PROTON FORM FACTORS,  $G_E$  AND  $G_M$ ,  
AT HIGH MOMENTUM TRANSFER AND THE QUESTION OF SCALING\*

S. C. Loken, B. C. Barish and J. Pine  
California Institute of Technology  
Pasadena, California

G. Buschhorn, † D. H. Coward, H. DeStaebler,  
J. Litt, L. W. Mo and R. E. Taylor  
Stanford Linear Accelerator Center  
Stanford University, Stanford, California

J. I. Friedman, G. C. Hartmann, †† and H. W. Kendall  
Massachusetts Institute of Technology  
Cambridge, Massachusetts

ABSTRACT

We report electron-proton elastic scattering cross sections measured at the Stanford Linear Accelerator Center at four-momentum transfers squared ( $q^2$ ) from 1.0 to 3.75 (GeV/c)<sup>2</sup>. The angular distributions at  $q^2 = 2.5$  and 3.75 (GeV/c)<sup>2</sup> allow a separation of the proton form factors,  $G_E$  and  $G_M$ . The measurements at lower  $q^2$  were taken at small angles and serve as a useful comparison with the previous external beam data from DESY. The measurements at 2.5 and 3.75 (GeV/c)<sup>2</sup> are compatible with scaling,  $G_E(q^2) = G_M(q^2)/\mu$ , within the experimental errors.

---

\* Work supported by the U.S. Atomic Energy Commission.

† Present address: DESY, Hamburg, Germany.

†† Present address: Xerox Corporation, Rochester, New York.

## INTRODUCTION

The scaling relationship between the electric ( $G_E$ ) and magnetic ( $G_M$ ) form factors of the proton is:

$$G_E(q^2) = G_M(q^2)/\mu \quad (1)$$

where  $\mu$  is the magnetic moment of the proton and  $q$  is the four-momentum transfer. This relation is true by definition in the limit of  $q^2 = 0$ , and has been shown<sup>1</sup> to hold within the experimental errors at  $q^2$  values up to  $1 \text{ (GeV/c)}^2$ .

At higher values of momentum transfer, the separation of  $G_E$  and  $G_M$  is more difficult as the contribution of  $G_E$  to elastic electron-proton scattering becomes less. In the one-photon exchange approximation, the Rosenbluth cross section for elastic electron-proton scattering is

$$\left(\frac{d\sigma}{d\Omega}\right) = \left(\frac{d\sigma}{d\Omega}\right)_{\text{NS}} \left\{ \frac{G_E^2 + \tau G_M^2}{1 + \tau} + 2\tau G_M^2 \tan^2 \frac{\theta}{2} \right\} \quad (2)$$

where

$$\left(\frac{d\sigma}{d\Omega}\right)_{\text{NS}} = \left(\frac{e^2}{2 E_0 \sin^2 \frac{\theta}{2}}\right)^2 \frac{E}{E_0} \cos^2 \frac{\theta}{2}$$

$$\tau = \frac{q^2}{4M^2}, \quad q^2 = 2 E_0 E (1 - \cos \theta)$$

in which  $E_0$ ,  $E$  are the incident and scattered energy of the electron,  $\theta$  is the electron scattering angle and  $M$  is the proton rest mass. The contribution of  $G_E$  is largest at small values of  $\theta$  and  $q^2$ . If we assume relation (1) to be true, the maximum percentage contribution of  $G_E^2$  to the cross section is 31% at  $q^2 = 1 \text{ (GeV/c)}^2$ , 15% at  $2.5 \text{ (GeV/c)}^2$  and 10% at  $4 \text{ (GeV/c)}^2$ .

The separation of the contributions of  $G_E$  and  $G_M$  is usually performed by measuring the angular distribution of electron-proton elastic scattering at a fixed value of four-momentum transfer and plotting the cross sections divided by  $(d\sigma/d\Omega)_{\text{NS}}$  versus

$\tan^2 \theta/2$ . The Rosenbluth cross section may be rewritten:

$$R_1 = I + S \tan^2 \theta/2 \quad (3)$$

where

$$\begin{aligned} R_1 &= (d\sigma/d\Omega)/(d\sigma/d\Omega)_{NS} \\ I &= (G_E^2 + \tau G_M^2)/(1 + \tau) \\ S &= 2 \tau G_M^2 \end{aligned}$$

Thus, as shown in Fig. 1a,  $G_M$  can be derived from the slope of  $R_1$  versus  $\tan^2 \theta/2$  and  $G_E$  can then be derived from the extrapolated intercept at  $\tan^2 \theta/2 = 0$ .

In the present paper we separate  $G_E$  and  $G_M$  using a slightly different treatment of the data. For convenience we normalize the form factors to the dipole model:

$$\left[ G_E(q^2) \right]_{\text{DIPOLE}} = \left[ G_M(q^2)/\mu \right]_{\text{DIPOLE}} = (1 + q^2/0.71)^{-2} \quad (4)$$

The dipole cross section,  $(d\sigma/d\Omega)_{\text{DIPOLE}}$ , is obtained by substituting Eq. (4) into Eq. (2). Thus we redefine the form factors at a fixed  $q^2$  value as:

$$\begin{aligned} g_E &= G_E (1 + q^2/0.71)^2 \\ g_M &= (G_M/\mu) (1 + q^2/0.71)^2 \end{aligned}$$

and define a kinematic factor,  $A$ , as:

$$A^{-1} = \mu^2 \tau \left[ 1 + 2(1 + \tau) \tan^2 \theta/2 \right]$$

where  $A$  varies from zero at  $\theta = 180^\circ$  to a maximum value ( $A_{\text{max}} = 1/\mu^2 \tau$ ) at  $\theta = 0^\circ$ .

Thus we may rewrite the Rosenbluth formula as:

$$R_2 = g_M^2 + A g_E^2 \quad (5)$$

where  $R_2 = (1 + A) (d\sigma/d\Omega)/(d\sigma/d\Omega)_{\text{DIPOLE}}$ .

This method of separating  $G_E$  and  $G_M$  is illustrated in Fig. 1b where  $g_E^2$  is the slope of  $R_2$  versus  $A$  and  $g_M^2$  is the extrapolated intercept. We see that if scaling is true the slope and intercept will be equal; and if the dipole relation is also true they will both equal unity. In this representation: (a) the statistical correlation between  $G_E$  and  $G_M$  is a little clearer, and (b) since  $g_E$  and  $g_M$  are  $G_E$  and  $G_M$  divided by the dipole predictions, small deviations from the dipole prediction are readily apparent.

At high  $q^2$  values the small size of the contribution of  $G_E$  to the cross section makes the separation of  $G_E$  and  $G_M$  very sensitive to the absolute normalization of an experiment. For this reason it is usual to extract the ratio  $(\mu G_E/G_M)$  from the data, as this quantity is insensitive to an absolute normalization provided all cross sections are changed by the same factor.

#### THIS EXPERIMENT

We have made angular distribution measurements of elastic electron-proton scattering at  $q^2 = 2.5$  and  $3.75$   $(\text{GeV}/c)^2$  which are sufficient to provide values of  $(\mu G_E/G_M)$  independent of the results from other laboratories. We also report small angle measurements at  $q^2$  values of  $1.0$ ,  $1.5$  and  $2.0$   $(\text{GeV}/c)^2$  which provide a useful check on the external beam measurements from DESY.<sup>2</sup>

An electron beam from the Stanford Linear Accelerator was momentum analyzed and passed through a 23-cm long liquid hydrogen target. The scattered particles were momentum analyzed using the SLAC 8-GeV/c magnetic spectrometer.<sup>3</sup> The particles were detected in two banks of scintillation counter hodoscopes located at the focal planes of the spectrometer. Scattered electrons were identified from the pulse height information from a lead-lucite total absorption shower counter. The incident beam currents were integrated using a toroid

induction monitor<sup>4</sup> and secondary emission monitors. Frequent intercalibrations were made using a Faraday cup,<sup>5</sup> which led us to regard the toroid as the main current monitor for the data runs, having typical fluctuations of only  $\pm 1/2\%$ . The experimental details and method of analysis were similar to that of previously reported elastic electron-proton measurements by this group.<sup>6</sup>

The highest  $q^2$  value was set at  $3.75 (\text{GeV}/c)^2$  due to the restricted angular range available to us for reasonable counting rates. Heating tests of our condensation-type liquid hydrogen target<sup>7</sup> showed that for average currents of about  $15 \mu\text{A}$  and beam spot sizes of a few square millimeters hydrogen density changes of about 20% could be induced. To be certain of keeping density changes below 1%, we restricted the average beam currents to below  $1 \mu\text{A}$  for the data runs. Our beam spot sizes were typically 3 mm high and 6 mm wide. The absolute density of the liquid hydrogen in the target cells is known to within about  $\pm 1-1/2\%$  from temperature and pressure measurements.

Care was taken to correct the data for angular dependent effects. The most important correction was for the variation of the spectrometer solid angle with momentum. A detailed check of the spectrometer optics was made by ray-tracing with electron beams of different momenta. Measurements at the focal planes were compared with beam transport computer predictions<sup>8</sup> which used first and second order matrix theory. The solid angle of the spectrometer varied by 2% over the momentum range of 1.7 - 8.0 GeV/c used for the data runs. A relative uncertainty of  $\pm 1/2\%$  is included in the experimental errors to allow for the accuracy in centering the elastic peak on the detectors. We assign an uncertainty of  $\pm 3\%$  to the absolute value of the solid angle.

The momentum dependence of the shower counter pulse height distribution has been studied together with the "signature" of the events from the counter hodoscopes. We feel that there remains an uncertainty in the final selection of events of about  $\pm 1\%$ .

The raw data have been corrected for radiative losses due to straggling of the electron beam in the target and thin windows<sup>9</sup> and losses due to bremsstrahlung in the scattering process.<sup>10</sup> For the latter, the formulae<sup>10</sup> of Tsai, and of Meister and Yennie have been applied, assuming exponentiation. Different analytic methods involving differential or integral radiative corrections have been used. We find that these different methods cause differences of  $\pm 1\%$  in the results at a given  $q^2$  value. The variation of the corrections with  $q^2$  led us to assign an absolute uncertainty of  $\pm 1\text{-}1/2\%$  to all cross sections.

The measured spectra after radiative correction have about 1% of the counts outside the expected elastic scattering peak. This amount varied from run to run and may reflect uncertainties in our empty target subtractions (which were typically 2 - 4%), or may be from pole-tip scattering in the spectrometer. This effect introduced an uncertainty of about one-fifth of the size of the errors in our form factor ratios at  $q^2 = 2.5$  and  $3.75$   $(\text{GeV}/c)^2$ .

The final cross section values are given in Table 1. Two runs performed at  $q^2 = 2.5$   $(\text{GeV}/c)^2$  were separated by several months and provide a useful check on the reproducibility of the data. Several runs have been combined at each angle and  $q^2$  value.

Table 1 contains only the relative errors which directly affect the ratio  $(\mu G_E/G_M)$ . These errors are due to counting statistics, empty target subtractions, fluctuations in beam monitoring ( $\pm 1/2\%$ ), density uncertainties of the hydrogen target ( $\pm 1\%$ ), uncertainties in the radiative corrections ( $\pm 1\%$ ) and solid angle ( $\pm 1/2\%$ ).

There is an overall systematic uncertainty (not included in the values given in Table 1) which is estimated to be about 4%. This includes the uncertainty in the absolute value of the solid angle ( $\pm 3\%$ ), beam monitor normalization ( $\pm 1/2\%$ ),

calibration of the incident energy and scattering angle ( $\pm 3/4\%$ ), the accuracy of the radiative corrections ( $\pm 1-1/2\%$ ), the uncertainty in data event selection ( $\pm 1\%$ ), and the density of the liquid hydrogen ( $\pm 1-1/2\%$ ). This error does not in good approximation affect the values of  $(\mu G_E/G_M)$  obtained with all-SLAC data as any normalization effect cancels in the ratio.

#### DISCUSSION OF RESULTS

Our data at  $q^2 = 1.0, 1.5$  and  $2.0$   $(\text{GeV}/c)^2$  are plotted in figures 2a - 2d together with the external beam data from Bonn<sup>11</sup> and DESY.<sup>2</sup> Systematic errors have not been included in the data. We have plotted the results according to the method outlined above (Eq. (5)). For each graph we have made minor adjustments to bring the data values to a central  $q^2$  value by applying the incremental change in the dipole cross section for each point.

At all  $q^2$  values, our data agree quite well with the DESY small angle measurements.<sup>2</sup>

In the figures 2a - 2d we include the published fits<sup>11</sup> to the combined Bonn and DESY data, and fits assuming that scaling (Eq. (1)) is true. The inclusion of systematic errors would reduce the significance of the deviations from scaling suggested by the data at  $q^2$  values of 1.16 and 1.50  $(\text{GeV}/c)^2$ . For example, a 1.5% normalization shift of the SLAC and DESY points relative to the Bonn data would change the ratio of  $(\mu G_E/G_M)$  by about 5% at these  $q^2$  values. The quoted systematic errors in the cross sections are 3.5% from Bonn,<sup>11</sup> 3% from DESY<sup>2</sup> and 4% from SLAC (this experiment). A comparison at  $q^2 = 0.6$   $(\text{GeV}/c)^2$  led to a difference in absolute normalization between Bonn and DESY of  $(+ 0.1 \pm 1.5)\%$ .<sup>11</sup>

At higher  $q^2$  values it becomes more difficult to make an accurate determination of the scaling ratio due to the expected small size of the contribution of  $G_E$ . In Fig. 2d at  $q^2 = 2.0 \text{ (GeV/c)}^2$  the Bonn and DESY combined data shows scaling within the experimental error of  $\pm 20\%$  in the ratio. A previous measurement by DESY<sup>12</sup> at  $q^2 = 3 \text{ (GeV/c)}^2$  found that scaling was true within the measurement error of  $\pm 24\%$ .

Our data at  $q^2 = 2.5 \text{ (GeV/c)}^2$ , shown as runs 1 and 2 in Fig. 2e, confirm scaling within the experimental error of  $\pm 19\%$ . At  $q^2 = 3.75 \text{ (GeV/c)}^2$  (Fig. 2f) scaling is found to be true within  $\pm 31\%$ .

In Fig. 3 we show the data from this experiment at  $q^2 = 2.5 \text{ (GeV/c)}^2$ , on a conventional Rosenbluth plot.

To summarize the present status of the scaling law in the range of  $q^2$  from  $1 - 4 \text{ (GeV/c)}^2$ , we plot in Fig. 4 the values of  $(\mu G_E/G_M)$  obtained from Refs. 11, 12 and from this experiment.

#### ACKNOWLEDGEMENTS

We would like to thank the accelerator crews, the target group and spectrometer facility group for their support during these measurements.

## REFERENCES

1. T. Janssens *et al.*, Phys. Rev. 142, 922 (1966).
2. W. Bartel *et al.*, Phys. Rev. Letters 17, 608 (1966).
3. L. Mo and C. Peck, "8-BeV/c spectrometer," Report No. SLAC-TN-65-29, Stanford Linear Accelerator Center, Stanford University, Stanford, California (1965) (unpublished); R. E. Taylor, Proceedings of the 1967 International Symposium on Electron and Photon Interactions at High Energies, Stanford Linear Accelerator Center, Stanford University, Stanford, California (1967), p. 78.
4. R. S. Larsen and D. Horelick, "A precision toroidal charge monitor for SLAC," Report No. SLAC-PUB-398, Stanford Linear Accelerator Center, Stanford University, Stanford, California (1968) (unpublished).
5. D. Yount, Nucl. Instr. and Methods 52, 1 (1967).
6. D. H. Coward *et al.*, Phys. Rev. Letters 20, 292 (1968).
7. R. L. Anderson, Nucl. Instr. and Methods 70, 87 (1969).
8. K. L. Brown, Report No. SLAC-75 (1967) and K. L. Brown, B. K. Kear and S. Howry, Report No. SLAC-91 (1969), Stanford Linear Accelerator Center, Stanford University, Stanford, California.
9. L. Eyges, Phys. Rev. 76, 264 (1949). We used Eq. (16) with  $a = 0.25$  and  $b = 1.333$ .
10. Y. S. Tsai, Phys. Rev. 122, 1898 (1961); N. Meister and D. R. Yennie, Phys. Rev. 130, 1210 (1963).
11. Chr. Berger *et al.*, Phys. Letters 28B, 276 (1968).
12. W. Bartel *et al.*, Phys. Letters 25B, 236 (1967).

### TABLE CAPTION

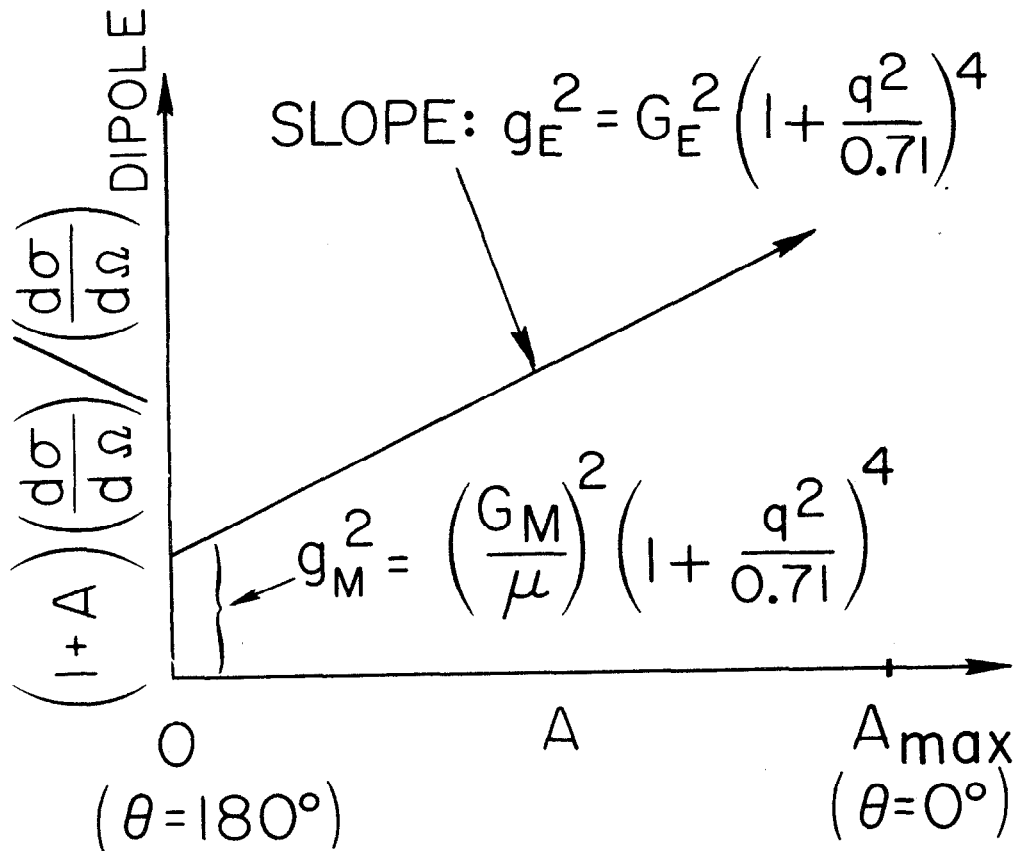
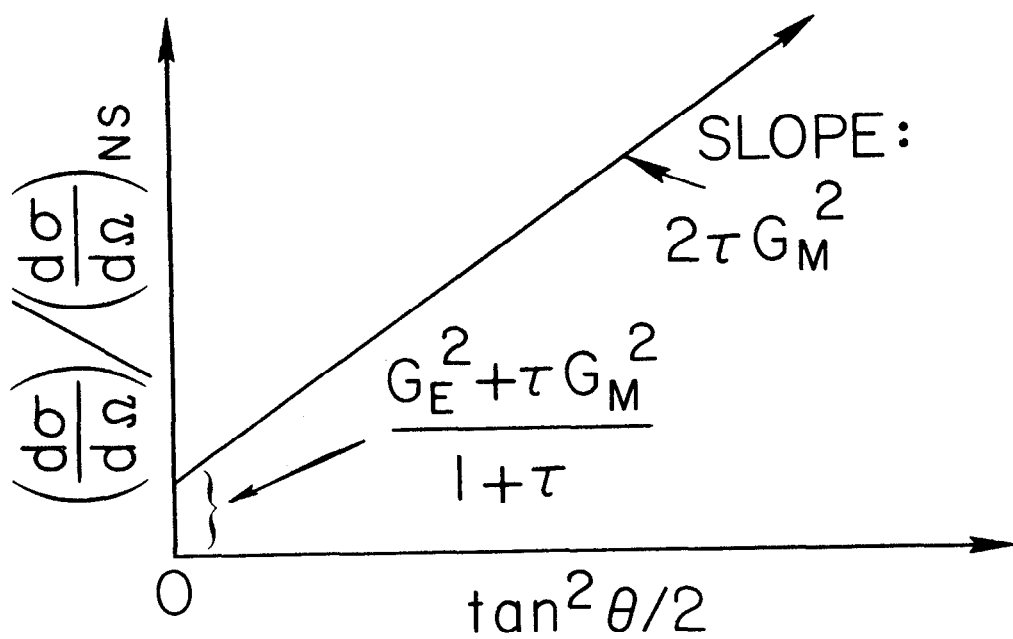
1. Final values of the electron-proton elastic scattering cross sections. Only random errors are shown. There is an overall systematic uncertainty, not included here, which we estimate to be  $\pm 4\%$ .

### FIGURE CAPTIONS

1. Two types of plots are illustrated which separate the contributions of the electric ( $G_E$ ) and magnetic ( $G_M$ ) form factors of the proton from electron-proton elastic scattering cross section data. 1a is the conventional Rosenbluth plot. 1b is a method which is described in the text.
2. a - f. Electron-proton elastic scattering data from Bonn,<sup>11</sup> DESY<sup>2</sup> and this experiment are shown on the type of plot illustrated in Fig. 1b. Systematic errors have not been included in the data. We include the published values<sup>11</sup> of  $(\mu G_E/G_M)$  for the combined Bonn and DESY measurements and fits assuming that the scaling relation  $G_E = G_M/\mu$  is true.
3. Data at  $q^2 = 2.5$  (GeV/c)<sup>2</sup> from this experiment are shown on a conventional Rosenbluth plot of  $(d\sigma/d\Omega)/(d\sigma/d\Omega)_{NS}$  versus  $\tan^2 \theta/2$ .
4. Values of  $(\mu G_E/G_M)$  from Refs. 11, 12 and this experiment are shown for the range of four-momentum transfer squared from 1 to 4 (GeV/c)<sup>2</sup>.

TABLE 1

$q^2$ (GeV/c) <sup>2</sup>	Incident energy $E_0$ (GeV)	Electron scattering angle $\theta$ (deg)	Final cross section $\frac{d\sigma}{d\Omega}$ (cm <sup>2</sup> /sr)
1.0	3.996	15.44	$(.6593 \pm .0092) \times 10^{-31}$
	3.296	19.06	$(.4065 \pm .0061) \times 10^{-31}$
	2.998	21.18	$(.3308 \pm .0051) \times 10^{-31}$
1.5	6.197	12.15	$(.3307 \pm .0049) \times 10^{-31}$
	3.296	24.64	$(.635 \pm .011) \times 10^{-32}$
	2.998	27.58	$(.4818 \pm .0075) \times 10^{-32}$
2.0	6.197	14.40	$(.830 \pm .014) \times 10^{-32}$
	3.996	23.84	$(.2414 \pm .0039) \times 10^{-32}$
	3.296	30.22	$(.1334 \pm .0032) \times 10^{-32}$
	2.998	34.14	$(.999 \pm .017) \times 10^{-33}$
2.5 (Run 1)	7.909	12.59	$(.4708 \pm .0067) \times 10^{-32}$
	5.253	20.09	$(.1538 \pm .0026) \times 10^{-32}$
	3.802	29.96	$(.565 \pm .010) \times 10^{-33}$
	3.294	36.20	$(.3532 \pm .0065) \times 10^{-33}$
2.5 (Run 2)	7.909	12.59	$(.4777 \pm .0066) \times 10^{-32}$
	6.197	16.55	$(.2566 \pm .0052) \times 10^{-32}$
	3.996	28.04	$(.688 \pm .012) \times 10^{-33}$
	3.296	36.17	$(.3475 \pm .0065) \times 10^{-33}$
	2.998	41.40	$(.2469 \pm .0045) \times 10^{-33}$
3.75	9.998	12.42	$(.973 \pm .014) \times 10^{-33}$
	7.911	16.26	$(.5112 \pm .0089) \times 10^{-33}$
	3.996	40.03	$(.4710 \pm .0092) \times 10^{-34}$



1392A6

Fig. 1

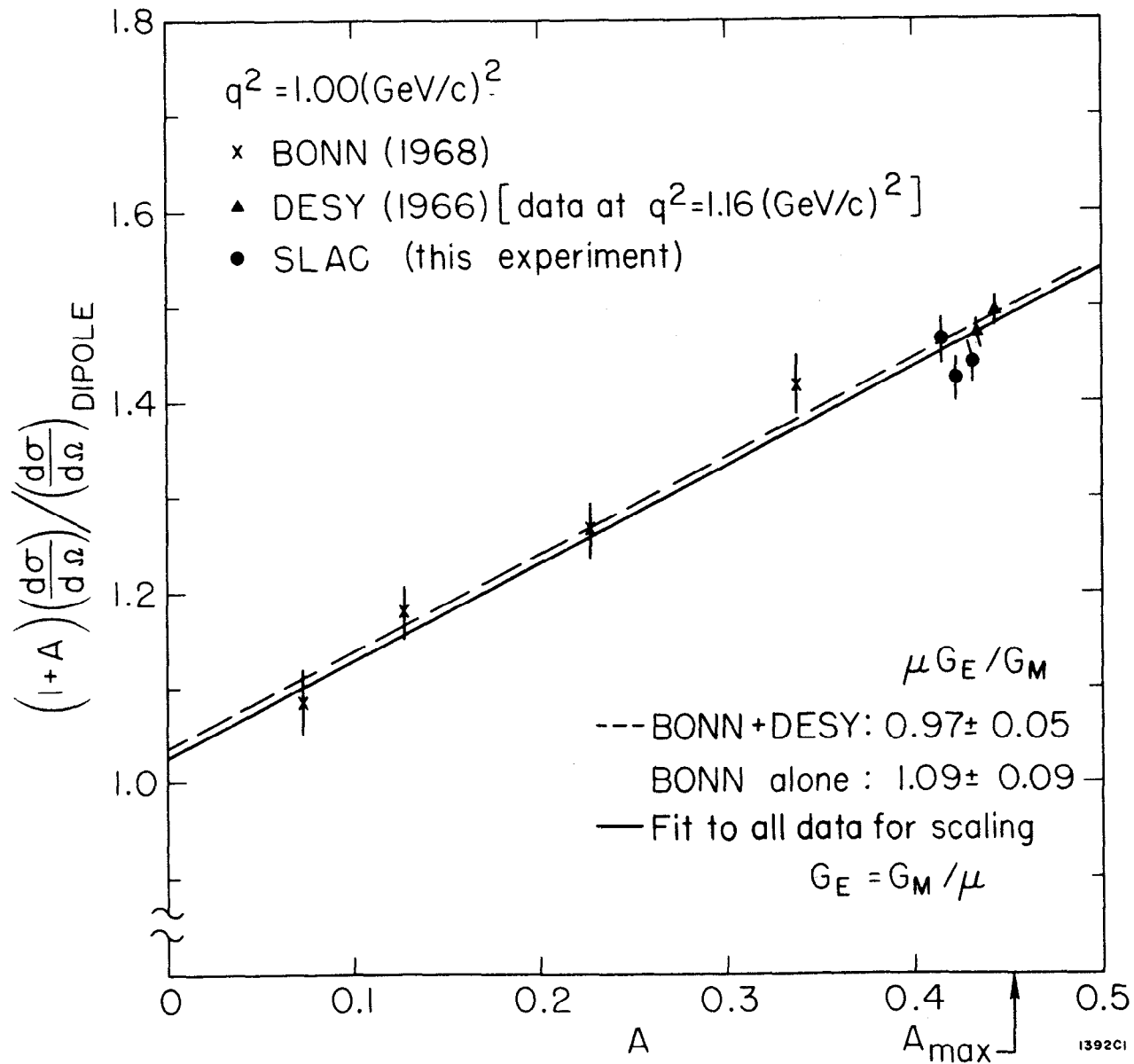


Fig. 2a

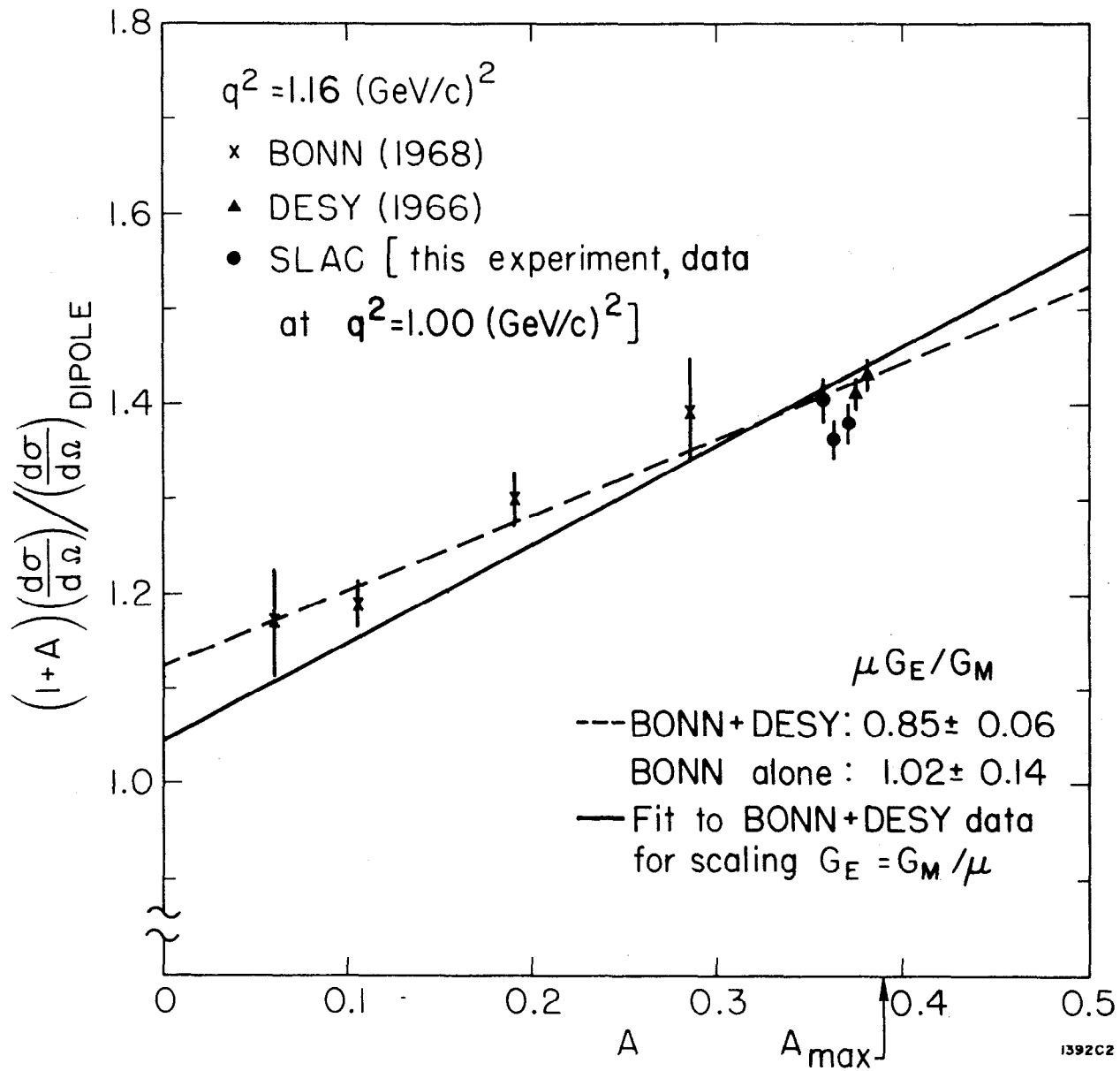


Fig. 2b

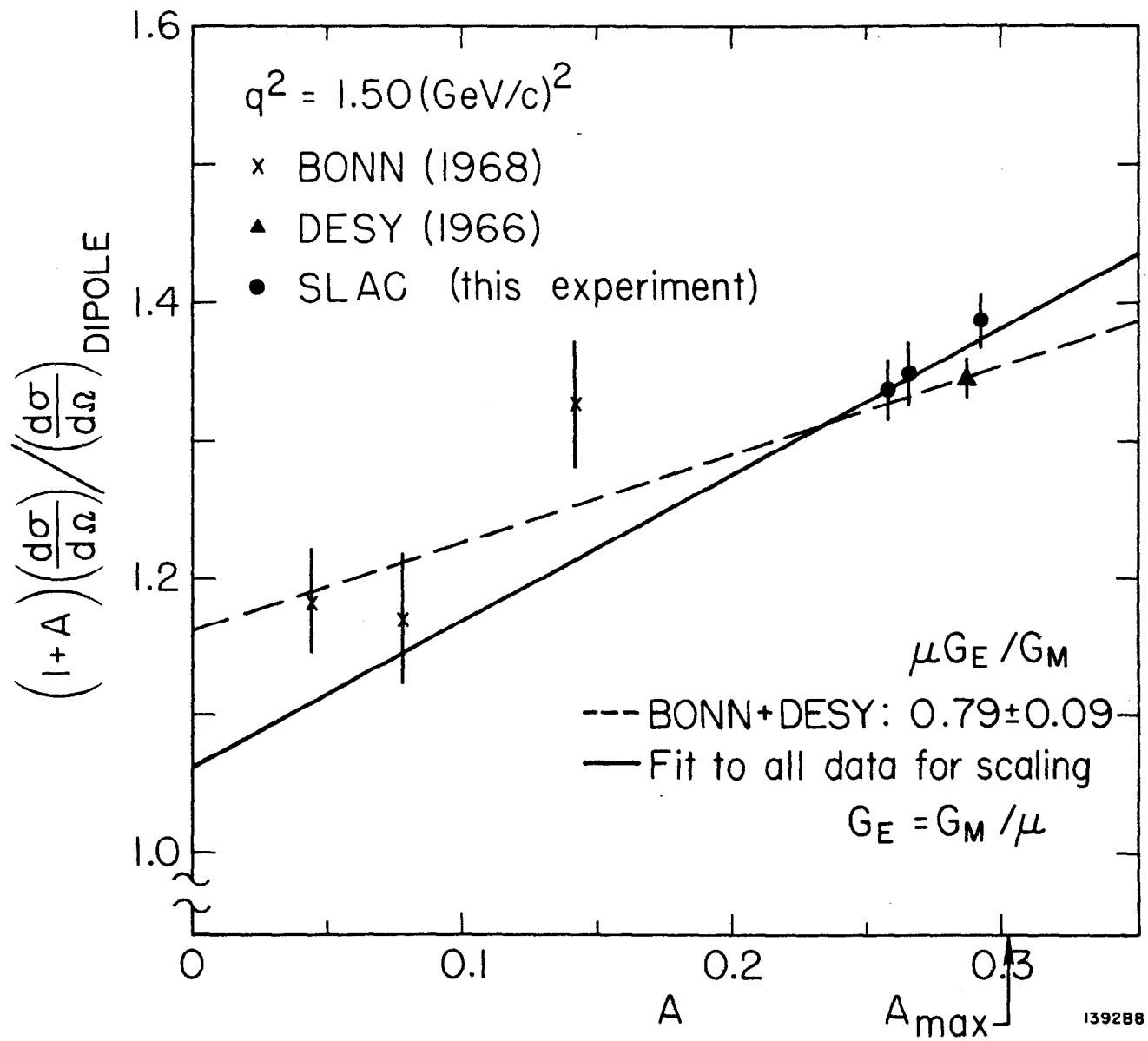


Fig. 2c

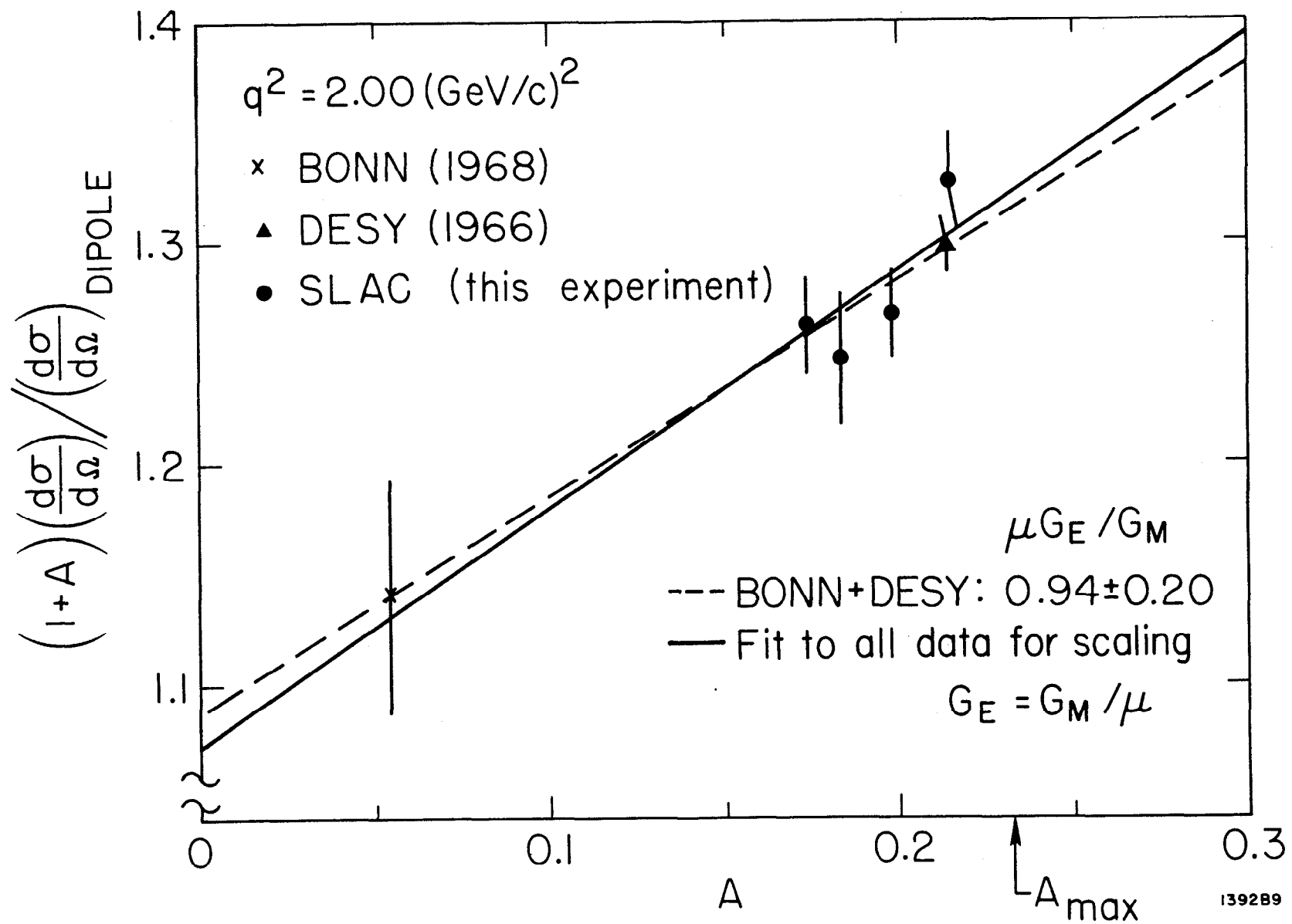
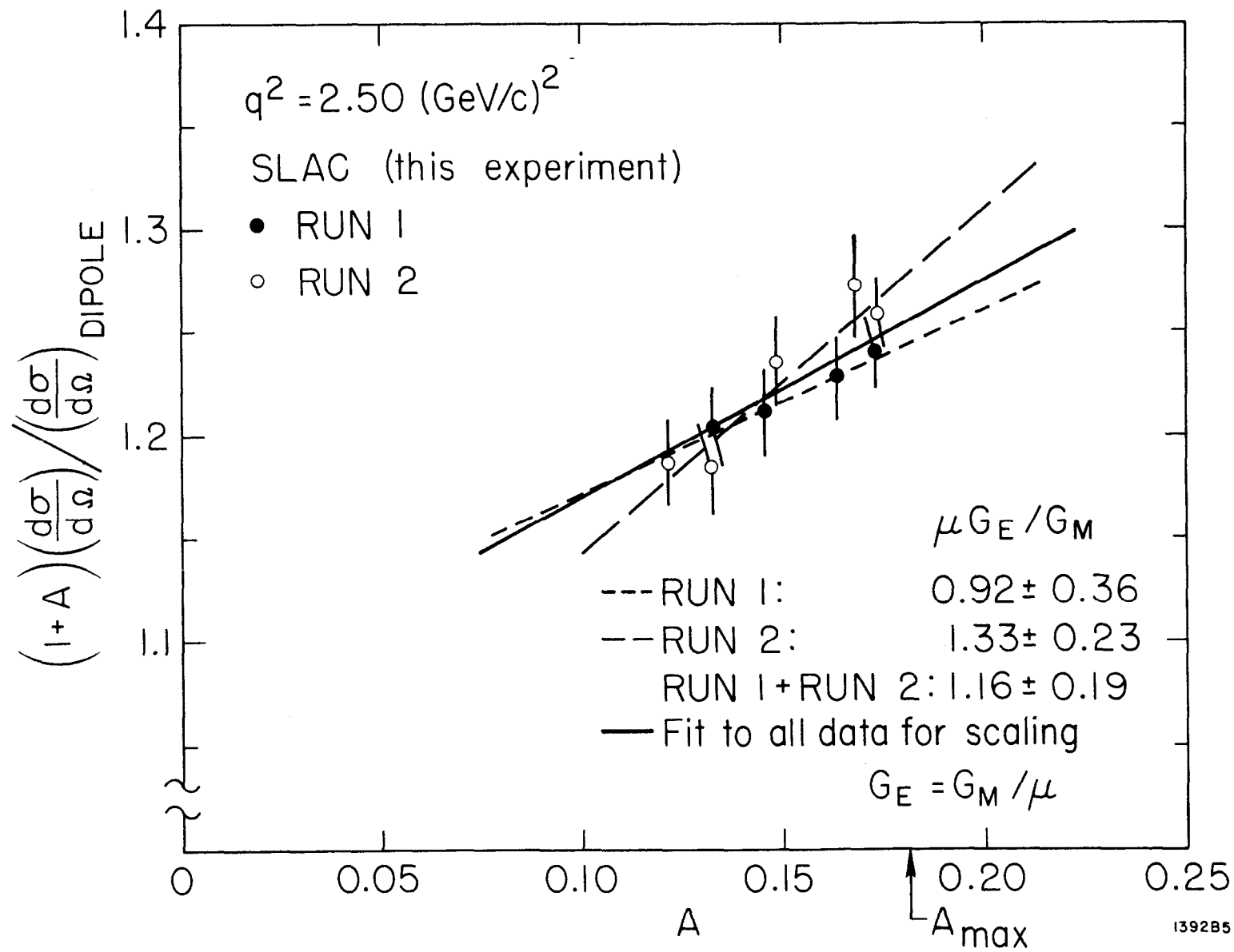


Fig. 2d



1392B5

Fig. 2e

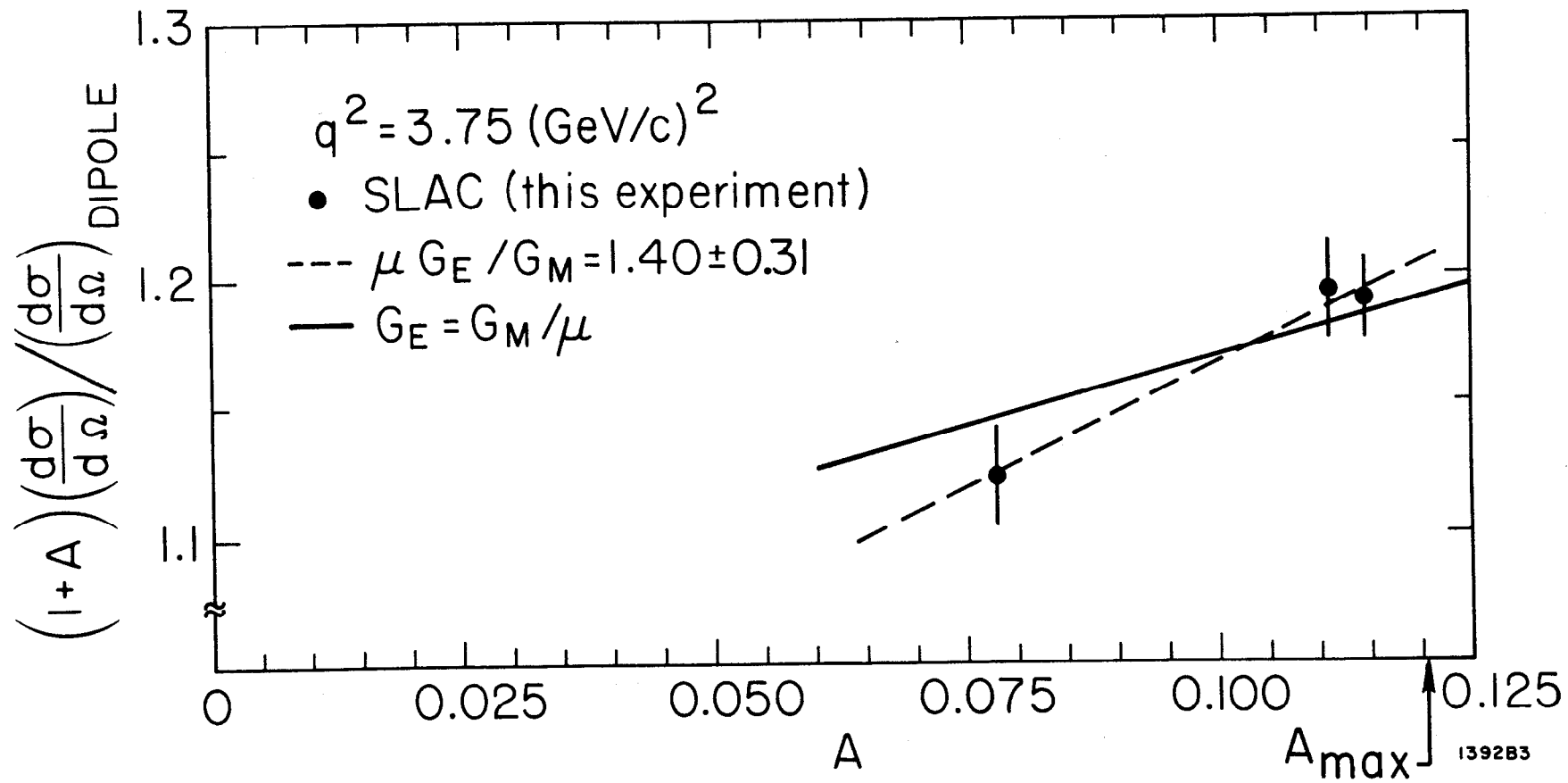


Fig. 2f

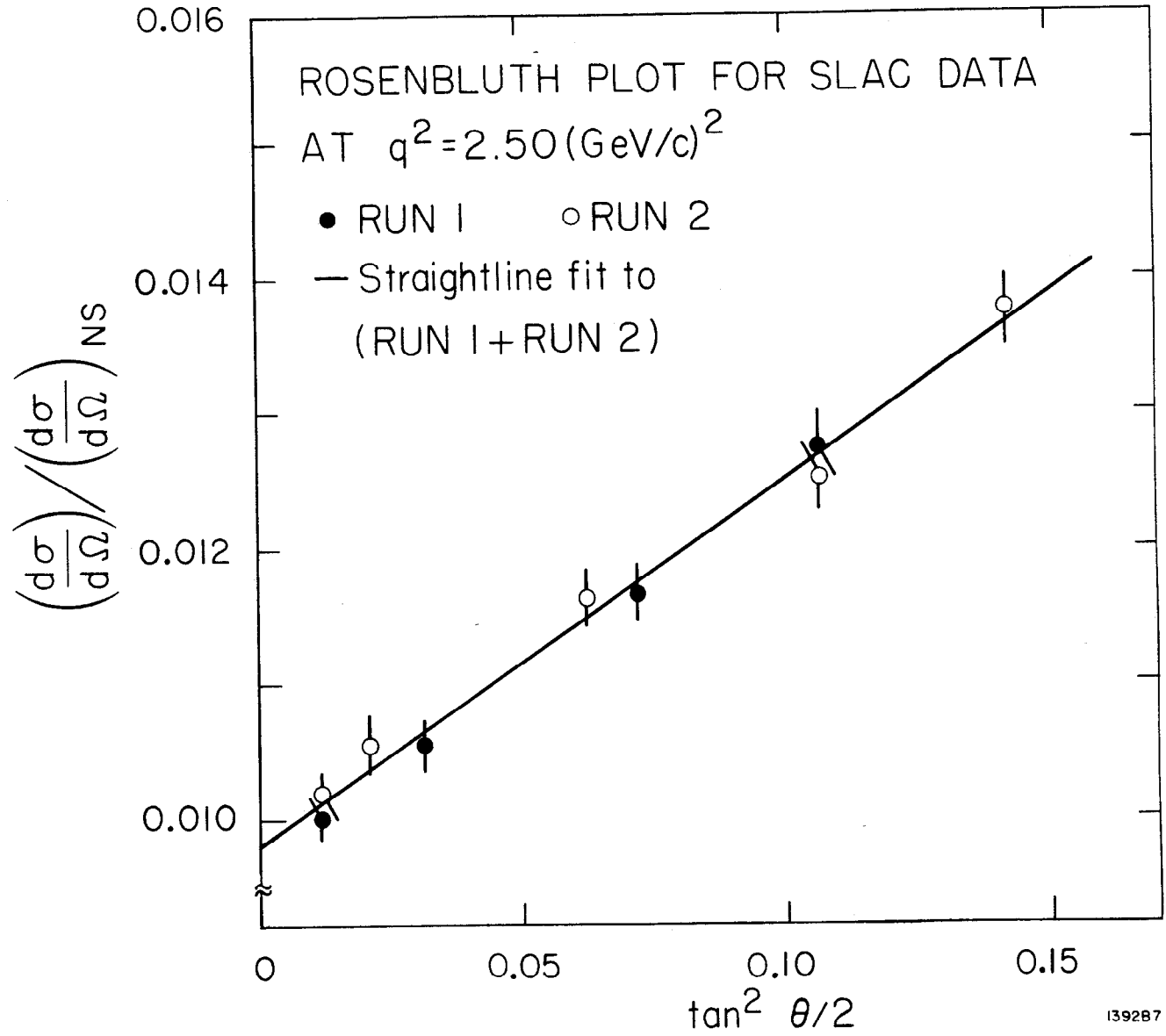
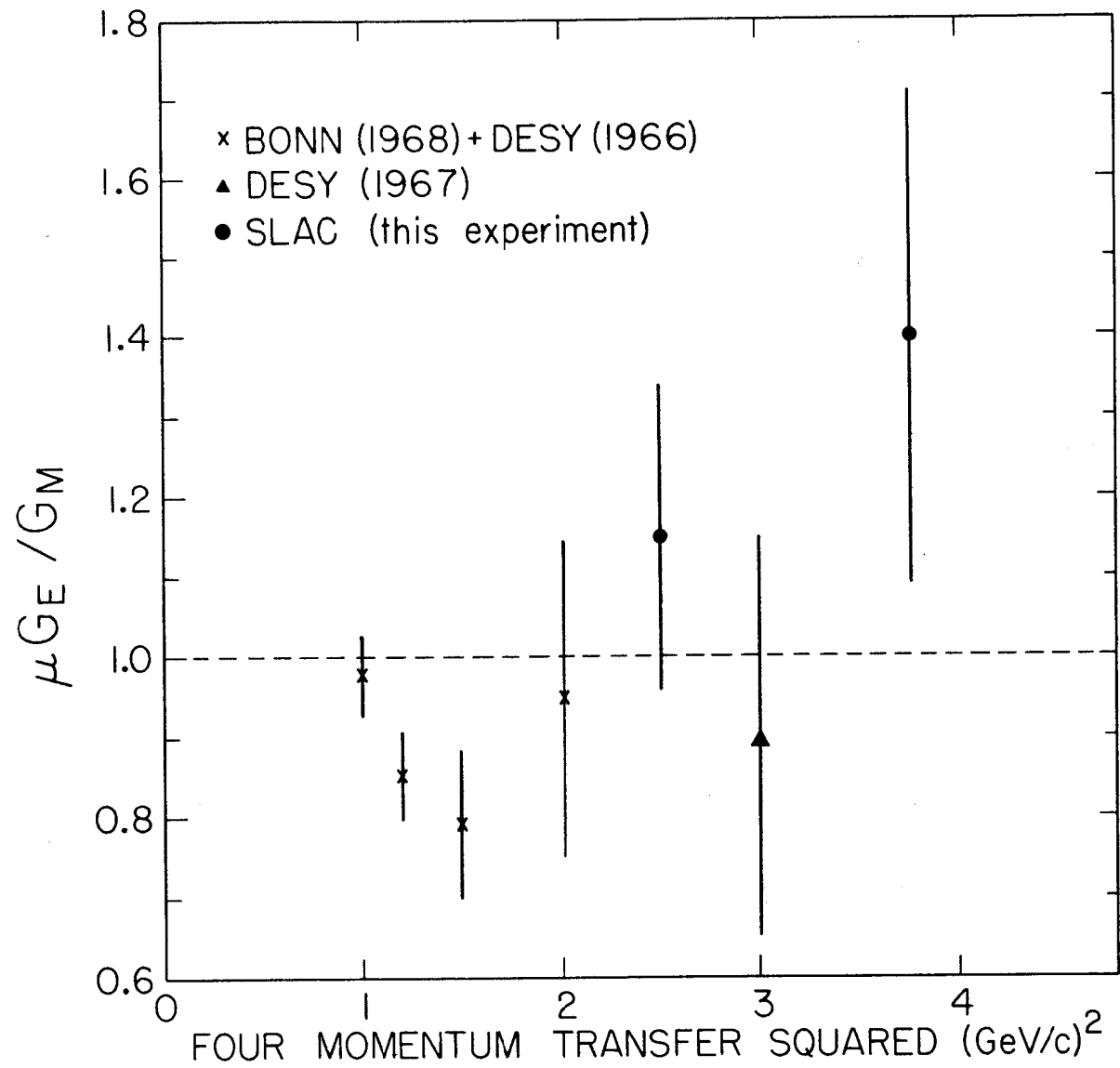


Fig. 3



1392C4

Fig. 4